SEMIEMPIRIC EQUATION OF STATE AND PHASE DIAGRAM OF TWO CONDENSE POLYSTYRENE PHASES

V. M. Elkin, V.N. Mikhaylov, T.Y. Mikhaylova

RFNC-VNIITF, Snezhinsk, Russia

Introduction

Polystyrene is a thermoplastic polymer of a preferentially linear structure with the repeating group $CH_2CH(C_6H_5)$ (molecular mass 104.15 g) [1]. Under ambient conditions it is in an amorphous vitreous state. Under shock loading polystyrene undergoes a physicochemical transformation (at a pressure of ~20 GPa) with considerable reductions in volume (~20%) and compressibility [2,3], and formation of a mixture of diamond-like carbon and low-molecular components [4]. In this paper the transformation is treated within the scope of first-order phase transition formalism with the low and high pressure phases denoted by α and β, respectively.

Parameters are chosen using thermophysical properties from quasi-static measurements [1, 5, 6] and data from shock experiments with solid and porous samples in a wide range of initial densities [2, 3, 7, 8]. Also used are calculations by the Thomas-Fermi method with Kopyshev Corrections (TFKC) for nuclear motion in homogeneous approximation [9, 10], and by Quantum Molecular Dynamics (QMD) [11].

Equation-of-state model

Our thermodynamically complete equation of state for polystyrene is constructed using a traditional representation of Helmholtz free (molar) energy in the form

$$F(V,T) = F_C(V) + F_A(V,T) + F_E(V,T) - T \cdot S_{tr}, \quad (1)$$

where V is molar volume, T is temperature, $F_C=E_C(V)$ is potential (cold) energy of atomic interaction at $T=0$ K; $F_A(V,T)$ and $F_E(V,T)$ are thermal contributions of atoms and thermally excited electrons to free energy. The last term $-T\cdot S_{tr}$ is used for describing the phase transition

The cold pressure in the compression region is written as [12]

$$P_C(y) = 3B_{0K}\frac{1-y}{y^5}\exp\left[C_0(1-y)\right]\left\{1 + C_1 y(1-y) + C_2 y(1-y)^2 + C_3 y(1-y)^3\right\}, \quad (2)$$

where $y = x^{1/3}$, $x = V/V_{0K}$, V_{0K} and B_{0K} are, respectively, the molar volume and the bulk modulus at $x = 1$. The potential free energy is determined by integrating $E_C(V) = E_{0K} - \int_{V_{0K}}^{V} P_C(V)dV$. Here E_{0K} is the value of cold energy at $x = 1$.

In the tension region $x > 1$, cold energy is defined in polynomial form

$$E_C(x) = V_{0K}\left[\frac{A}{m}\left(x^{-m}-1\right) + \frac{B}{n}\left(x^{-n}-1\right) + \frac{C}{k}\left(x^{-k}-1\right)\right] + E_{0K}, \quad (3)$$

which gives an equation for pressure in the form

$$P_C(x) = Ax^{-(1+m)} + Bx^{-(1+n)} + Cx^{-(1+k)}. \quad (4)$$

The parameters in Eq. (3) are related to sublimation energy by $\frac{A}{m} + \frac{B}{n} + \frac{C}{k} = -\frac{E_{sub}}{V_{0K}}$. Equations (2) and (4) for pressure are joined with their first and second derivatives with respect to volume at $x = 1$, which poses certain conditions on the parameters: $A+B+C = 0$, $mA + nB + kC = B_{0K}$, $m^2A + n^2B + k^2C = (B'_{0K} - 2)\cdot B_{0K}$. The parameters k and m are free (adjustable).

The thermal free energy of ions is written as a superposition of Debye and Einstein contributions with different characteristic temperatures

$$F_a(V,T) = w_D F_D(V,T) + \sum_i w_{Ei} F_{Ei}(V,T), \quad (5)$$

$$F_D(V,T) = RT\left\{\frac{9}{8}\tau_D + 3\ln\left[1-\exp\left(-\tau_D\right)\right] - D\left(\tau_D\right)\right\}, \quad (6)$$

$$F_{Ei}(V,T) = 3RT\ln\left[1-\exp\left(-\tau_{Ei}\right)\right], \quad (7)$$

$\tau_D = \frac{\sqrt{\theta_D^2+\theta_G^2}}{T}$, $\tau_{Ei} = \frac{\sqrt{\theta_{Ei}^2+\theta_G^2}}{T}$, $\theta_G(V,T) = \lambda^{-1/3}T^{1/2}$, $D(\tau) = \frac{3}{\tau^3}\int_0^\tau \frac{x^3 dx}{e^x-1}$, is Debye function, w_D, w_{Ei} are fractions of degrees of freedom $w_D + \sum_i w_{Ei} = 1$, λ is an adjustable parameter. Equation (5) with characteristic temperature in the form $\theta = \sqrt{\theta_{D,E_i}^2+\theta_G^2}$ [10] describes a solid at low temperatures ($\theta \approx \theta_{D,E_i}$) and an ideal atomic gas at high temperatures ($\theta \approx \theta_G$).

The Gruneisen function is taken in the form of empirical relation [13]

$$\Gamma(V) = \frac{2}{3} + \frac{\left(\Gamma_0 - \frac{2}{3}\right)\left(B^2+D^2\right)}{B^2+\left(D-\ln x\right)^2}, \quad (8)$$

where Γ_0 is Gruneisen parameter at x =1, B and D are adjustable coefficients.

The electron free energy is defined as [13]

$$F_E(V,T) = -C_E(V,T)T\ln\left[1+\frac{B_E(T)T}{2C_{Ei}}x^{\Gamma_E(V,T)}\right], \quad (9)$$

where $B_E(T) = \frac{2}{T^2}\int\left[\int_0^T \beta(\tau)d\tau\right]dT$, $\tilde{N}_{Ei} = \frac{3RZ}{2}$. Equation (9) contains generalized analogs of:

heat capacity of electron gas

$$C_E(V,T) = \frac{3R}{2}\left[Z + \frac{T_Z^2(1-Z)x}{(x+x_Z)\left(T^2+T_Z^2\right)}\right]\exp\left(-\frac{\tau_i}{T}\right), \quad \tau_i = T_i\exp\left(-\frac{x}{x_i}\right), \quad (10)$$

Gruneisen coefficient of electrons

$$\Gamma_E(V,T) = \Gamma_{Ei} + \left(\Gamma_{E0} - \Gamma_{Ei} + \gamma_m\frac{T}{T_g}\right)\exp\left(-\frac{T}{T_g}\right), \quad (11)$$

and electron heat coefficient

$$\beta(T) = \beta_i + \left(\beta_0 - \beta_i\right)\exp\left(-\frac{T}{T_b}\right). \quad (12)$$

Parameters for the equations of state were chosen with a genetic algorithm [14] from the condition of optimal fit to experimental and theoretical data.

Comparison between calculated and experimental data

Adequacy of the free energy function and parameters used is illustrated below by comparing EOS calculations with experimental data and calculations with theoretical models.

Calculated and experimental (in brackets) values of density ρ =1.05 (1.05 [1]) g/cm^3, volumetric thermal expansion coefficient β_D = 2.04·10^{-4} K^{-1} (2.0·10^{-4} K^{-1} [1]), and adiabatic bulk modulus B_S = 3.78 (3.77 [3]) GPa under ambient conditions (for the α phase), and the thermal behavior of specific heat (at P=0 *GPa*) agree well. The isobaric decrease of the isothermal modulus with temperature ends at 804 K where it

becomes zero, which points to the fact that the isobar crosses the spinodal – the line of absolute instability. The resulted value on the spinodal agrees with the experimental value ~ 805 K [6].

Figure 1 shows Hugoniots for single- and two-stage compressions of solid material at pressures below 160 GPa and at ultrahigh pressures in the insertion. Calculations are compared with experimental data for single- [2, 3] and two-stage [7] compressions (the state behind the front of the first wave is characterized by

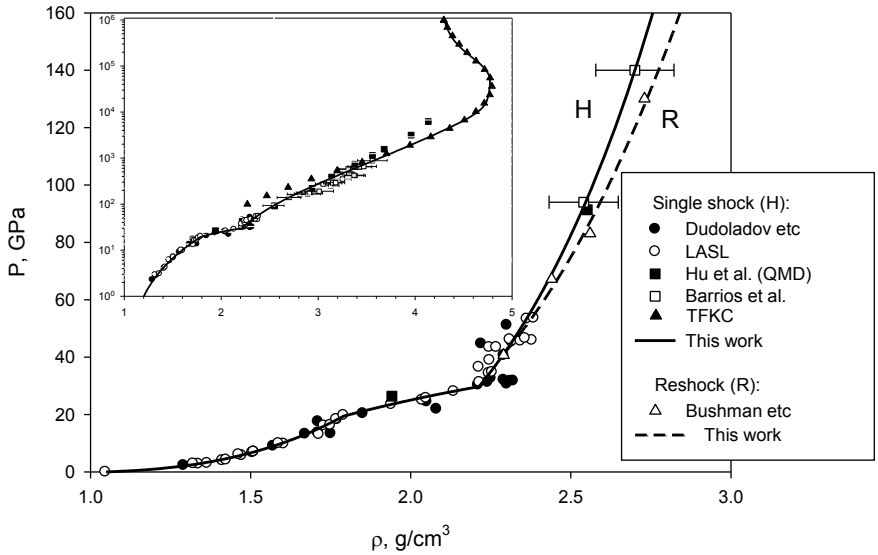

Figure 1. Hugoniots of single- (H) and two-stage (R) compressions at pressures below 160 GPa (calculated and experimental data from [2, 3, 7, 8, 11])

Breaks on the Hugoniot in the range of pressures between 20 and 30 GPa (see Fig. 1) are caused by the physicochemical transformation of polystyrene. The calculated points where the transition starts and ends (in brackets) are: P_{tr} = 19.4 (29.7) GPa, ρ_{tr} = 1.79 (2.21) g/cm^3, T_{tr} = 1370 (2229) K. The phase transition occurs with no phase precursor.

The experimental Hugoniots of porous polystyrene [2, 3] in the $\rho - P$ coordinates are characterized by a large spread. That is why in Fig.2 they are shown in the U – P coordinates in comparison with calculated results. The figure also shows Hugoniots for singe- [2, 3] and two-stage [7] compressions of solid polystyrene, and isentropes of unloading from the state P = 40.7 GPa, U = 4.58 km/s, calculated with the EOS for the β phase. Calculation with account for the phase transition reproduces experimental data much worse, which suggests that the diamond-like β phase recovers (within the scopes of the EOS) in unloading. Here the analogy with the formation of diamonds from explosion products and their recovery after unloading seems to be quite in place. Note that the last experimental point (P = 0.2 GPa) on the calculated unloading curve is in the spinodal bounded region where the condensed phase is absolutely unstable thermodynamically. The experimental Hugoniots of porous polystyrene with initial densities ρ_{00} = 0.7, 0.5 g/cm^3 correspond to the EOS of α polystyrene. At ρ_{00} = 0.3 g/cm^3, the difference in the description of experimental data by the equations of state for α and β phases is still present, while at densities between 0.055 and 0.2 g/cm^3, it almost vanishes (no higher than the thickness of lines, see insertion in Fig.2).

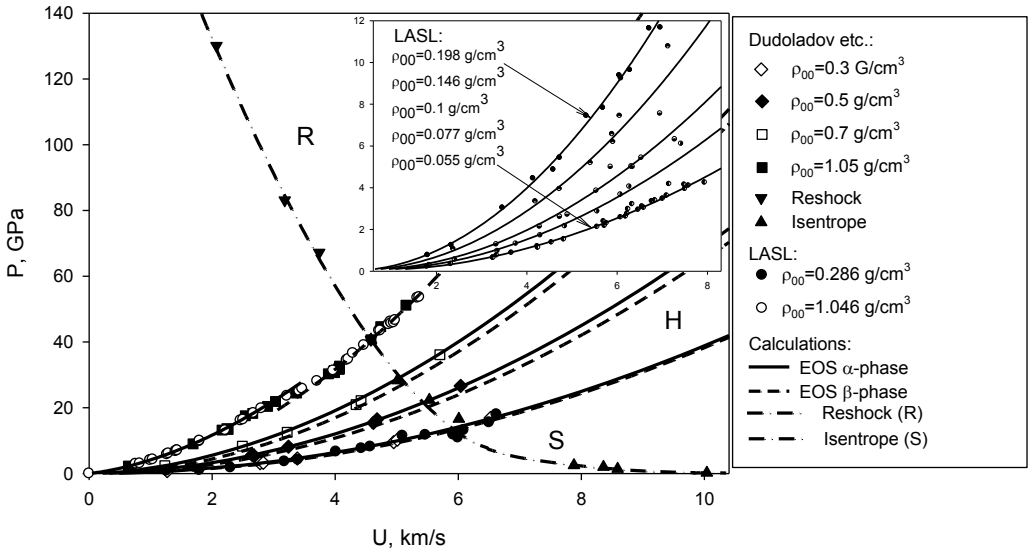

Figure 2. Hugoniots for different initial densities (H), two-stage compression Hugoniot (R), and expansion isentrope (S); experimental data from [2, 3, 7]

Experimental data on the line of the α - β transition are absent in the literature. The phase diagram proposed in this paper

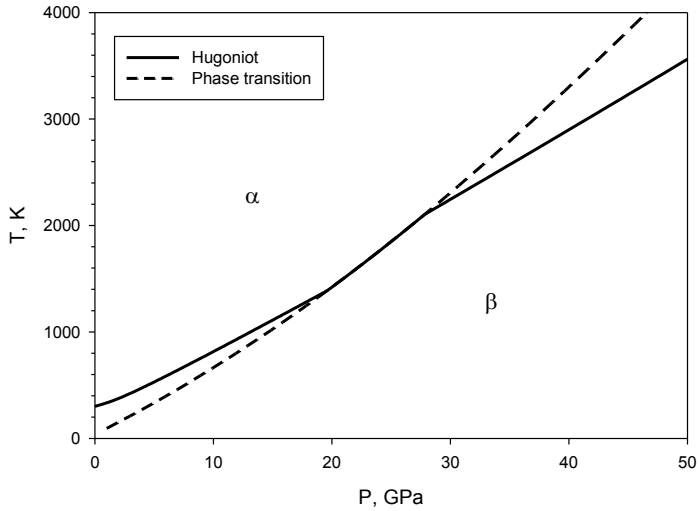

Figure 3. Phase diagram of polystyrene

We first calculated Hugoniot temperatures corresponding to the beginning and end of the transition. These points are quite distinct on the experimental Hugoniot. Then, from the equality of thermodynamic potentials of the two phases, we constructed the line of phase equilibrium through these points so as to satisfy the following additional conditions. First, the (P – T) states of the Hugoniots for porous material, which are well described by the EOS of the α phase (ρ_{00} = 0.3 - 0.7 g/cm^3) but not described by the EOS of the β phase, must be in the phase diagram region corresponding to the α phase which is only possible is the slope dT/dP of the transformation curve is positive in the range of pressures 20-36 GPa. Second, the phase equilibrium line must monotonically increase for not to allow the reverse β - α transformation to occur at pressures up to 100 GPa at least. These conditions were satisfied through optimization of values for the parameters E_{0K}, S_{tr}, $\theta^{\beta}_{0E_1}$ and $w^{\beta}_{E_1}$.

Our phase diagram for polystyrene significantly differs in the slope of the transition curve from the diagram of phenylene proposed in [15], where the equations of state for polystyrene, polyimide and phenylene are constructed with account for physicochemical transformations that occur in these polymers.

The phase diagram presented only for phenylene has a positive slope at pressures below ~2.5 GPa, but at higher pressures the slope becomes negative. It is proposed that the other aromatic polymers have similar phase diagrams. This disagrees with our results. The disagreement could be resolved through the reliable determination of transition pressure in additional experiments with porous samples.

Conclusion

We have proposed a semiempirical equation of state for two polystyrene phases. The equation is fit to data from static and dynamic experiments. The polystyrene Hugniots from calculations agree well with experimental measurements in the entire range of studied pressures (up to ~ 1000 GPa) and temperatures (up to ~ 10^5 K), and with calculations by the TFKC model beyond the range. Good agreement is also obtained with shock compression data for porous polystyrene in a wide range of initial densities from 1.05 to 0.055 g/cm^3. Proposed is a phase diagram which separates the regions where the low- and high-pressure phases exist.

References

1. V.A. Kargina, Encyclopedia of polymers. Moscow, // Soviet Encyclopedia Publishers, 1972, V.1, 1224 p., V.2, 1032 p., V.3, 1152 p.
2. I.P. Dudoladov, V.I. Rakitin, Y.N. Sutulov, and G.S. Telegin, // J. Applied Mechanics and Engineering Physics, 1969, No. 4, P. 148-151.
3. S.P. Marsh, Shock Hugoniot Data. Los Alamos series on dynamic material properties //University of California Press, 1980, 658 p.
4. F.H. Ree // J. Chem. Phys. 70, 974 (1979).
5. B. Wunderlich, and H. Baur, Heat capacities of linear high polymers. // Moscow, MIR Publishers, 1972, 237 p.
6. K.V. Khishenko, I.V. Lomonosov, V.E. Fortov, and O.F. Shlensky, // Proceedings of Academy of Sciences, V.349, No.3, P.322-325 (1996).
7. A.V. Bushman, M.V. Zhernokletov, I.V. Lomonosov, Y.N. Sutulov, V.E. Fortov, and K.V. Khishenko, // J. Experimental and Theoretical Physics, V.109, Is. 5, P.1662-1670 (1996).
8. M.A. Barrios, D.G. Hicks, T.R. Boehly, D.E. Fratanduono, J.H. Eggert, P.M. Celliers, G.W. Collins, D.D. Meyerhofer // Phys. Plasmas 17, 056307 (2010).
9. V.P. Kopyshev, Preprint 59 of the Institute of Applied Mathematics of Academy of Sciences, Moscow, 1978.
10. V.P. Kopyshev, The theory of equations of state. RFNC-VNIIEF, Sarov, 2009.
11. S.X. Hu, T.R. Boehly, L.A. Collins // Phys. Rev. E 89, 063104(2014).
12. W.B. Holzapfel //Phys. Rev. B. V.67, 026102(2003); J.S. Tse, W.B. Holzapfel //J. Appl. Phys. V.104, 043525 (2008).
13. L.V. Altshuler, A.V. Bushman, M.V. Zhernokletov, V.N. Zubarev, A.A. Leontiev, and V.E. Fortov, // J. Experimental and Theoretical Physics, Is. 2, P.741-760 (1980).
14. V.N. Mikhaylov, V.M. Elkin, and T.Y. Mikhaylova, // RFNC-VNIITF Preprint 232, Snezhinsk, 2007.
15. K.V. Khishenko, V.E. Fortov, I.V. Lomonosov // Int. J. Thermophys. 23, No.1, P.211-219 (2002).

МОДЕЛИРОВАНИЕ ТЕРМОДИНАМИЧЕСКИХ ПАРАМЕТРОВ СМЕСЕЙ С КОМПОНЕНТАМИ, ИСПЫТЫВАЮЩИМИ ФАЗОВЫЙ ПЕРЕХОД ПРИ УДАРНО-ВОЛНОВОМ ВОЗДЕЙСТВИИ

К.К. Маевский, С.А. Кинеловский

Институт гидродинамики СО РАН им. М.А. Лаврентьева, Новосибирск, Россия

Ударно-волновой синтез и компактирование с использованием порошковых смесей являются перспективным направлением создания новых материалов. Интенсивные исследования сжимаемости смесей для создания материалов с необходимыми свойствами, в частности